Transport suppression in non-monotonic zonal flows including finite Larmor radius

D. del-Castillo-Negrete[1], J. J. Martinell[2]

[1] *Oak Ridge National Laboratory, Oak Ridge, TN 37831-6169, USA*

[2] *Instituto de Ciencias Nucleares, UNAM, MEXICO*

I. Introduction

The relationship between transport and shear is a problem of considerable interest in magnetically confined plasmas. It is well known that there are cases in which an increase of flow shear can lead to a reduction of *turbulent* transport. However, this is not a generic result, and there are transport problems in which the opposite is the case. In particular, barriers to *chaotic* transport can form in regions of vanishing shear [1,2]. This property, which is generic to the so-called non-twist Hamiltonian systems [3] explains the observed resilience of transport barriers in non-monotonic zonal flows in plasmas and fluids and the robustness of shearless magnetic surfaces in reverse shear configurations. Here we study the role of finite Larmor radius (FLR) effects on chaotic transport in non-monotonic shear flows.

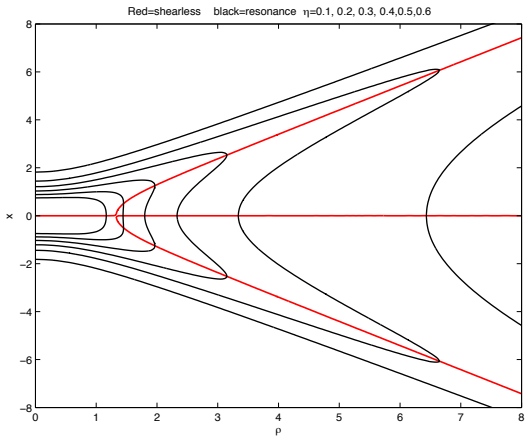

Figure 1: Zonal flow bifurcation due to FLR effects. The red curves indicate the location of the shearless transport barrier(s). The black curves denote the location of the critical layer resonance for different mode phase velocities, $\eta = 0.6, 0.5, 0.4, 0.3, 0.2$ and 0.1.

II. Test particle transport model

When FLR effects can be neglected, test particle transport is governed by the guiding center equations of motion. In the $\mathbf{E}\times\mathbf{B}$ approximation with $\mathbf{B} = B_0\hat{\mathbf{z}}$, and $\mathbf{E} = -\nabla\phi(x,y,t)$ the equations correspond to a Hamiltonian dynamical system with (x,y) playing the role of canonically conjugate variables and ϕ playing the role of the Hamiltonian. To incorporate FLR effects we gyroaverage the $\mathbf{E}\times\mathbf{B}$ Hamiltonian system [4]

$$\frac{dx}{dt} = -\left\langle \frac{\partial\phi}{\partial y}\right\rangle_\theta, \qquad \frac{dy}{dt} = \left\langle \frac{\partial\phi}{\partial x}\right\rangle_\theta \tag{1}$$

where the gyroaverage, $\langle\rangle_\theta$, is defined as $\langle\Psi\rangle_\theta \equiv \frac{1}{2\pi}\int_0^{2\pi}\Psi(x+\rho\cos\theta, y+\rho\sin\theta)\,d\theta$. This

is a good approximation provided the gyrofrequency is greater than other frequencies in the system.

Following [1,2] we assume the system is near marginal stability and model ϕ as a superposition of regular neutral modes of the Hasegawa-Mima equation. As a paradigmatic example of non-monotonic zonal shear flows we consider $\hat{u}_0(x) = \mathrm{sech}^2 x$ for which the Hamiltonian for two modes (in the co-moving reference frame of mode 1) is

$$\phi = \tanh x - \eta x + \varepsilon_1 \mathrm{sech}^2\mathrm{x}\cos(\mathrm{k_1 y}) + \varepsilon_2 \mathrm{sech}^2\mathrm{x}\cos(\mathrm{k_2 y} - \omega\mathrm{t}) \,. \tag{2}$$

Substituting Eq. (2) into (1) and doing the gyroaverage leads to the following test particle model for chaotic transport including finite Larmor radius effects

$$\begin{aligned} \tfrac{dx}{dt} &= \varepsilon_1 k_1 I_{k_1,\rho}(x)\sin k_1 y + \varepsilon_2 k_2 I_{k_2,\rho}(x)\sin(k_2 y - \omega t) \,, \\ \tfrac{dy}{dt} &= I_{0,\rho}(x) - \eta - 2\varepsilon_1 K_{k_1,\rho}(x)\cos k_1 y - 2\varepsilon_2 K_{k_2,\rho}(x)\cos(k_2 y - \omega t) \,. \end{aligned} \tag{3}$$

where

$$I_{k,\rho}(x) = \frac{1}{\pi}\int_0^\pi \mathrm{sech}^2(\mathrm{x} - \rho\cos\theta)\cos(\mathrm{k}\rho\sin\theta)\,\mathrm{d}\theta \,, \tag{4}$$

$$K_{k,\rho}(x) = \frac{1}{\pi}\int_0^\pi \mathrm{sech}^2(\mathrm{x} - \rho\cos\theta)\tanh(\mathrm{x} - \rho\cos\theta)\cos(\mathrm{k}\rho\sin\theta)\,\mathrm{d}\theta \,, \tag{5}$$

III. Zonal flow and streamline topology bifurcations For $\rho = 0$ the zonal flow has a single maximum since the velocity field has a simple $\mathrm{sech}^2\mathrm{x}$ dependence. However, as ρ increases the flow $u_0(x) = I_{0\rho}(x)$ exhibits a bifurcation leading to additional extrema, which are related to shearless barriers. Fig.(1) tracks the location of the zonal flow shearless barriers defined as $\sigma_0(x;\eta,\rho) = \partial^2\langle\phi\rangle_\theta/\partial x^2 = -2K_{0\rho}(x) = 0$. For $\rho \leq 1.33$ there is only one shearless region (single maximum of u_0) and for larger ρ there is a bifurcation (two maxima and a central minimum). The first step to understand the effect of normal modes on transport is to study the location of the resonances located where the propagation velocity of the mode matches the velocity of the zonal flow. For a single mode, these are defined by $I_{0\rho}(x) - \eta = 0$ and are shown in Fig.(1) with solid black lines for several values of η.

As discussed in [1,2], in the case $\rho = 0$, the streamlines (iso-contours of ϕ) can exhibit separatrix reconnection which is a global change in the phase space topology. For the case of symmetric zonal flows the topology can change for heteroclinic (in which two hyperbolic points are joined by the separatrix) to homoclinic (in which the separatrix joins the stable and unstable manifolds of the same hyperbolic point). The FLR effects play a very interesting role in separatrix reconnection. In particular, it is observed that as the Larmor radius increases, the topology of the Hamiltonian changes from the heteroclinic topology for small values of ρ to the homoclinic

topology at intermediate values of ρ. Moreover, in the case for large enough ρ, the trapping regions around the elliptic fixed points disappear and the dynamics is dominated by a strong wavy parallel zonal flow.

It is also interesting to observe that, as Fig. 2 shows, for parameter values for which the zonal flow has bifurcated and created two maxima (see Fig. 1) it is possible to have double separatrix reconnection.

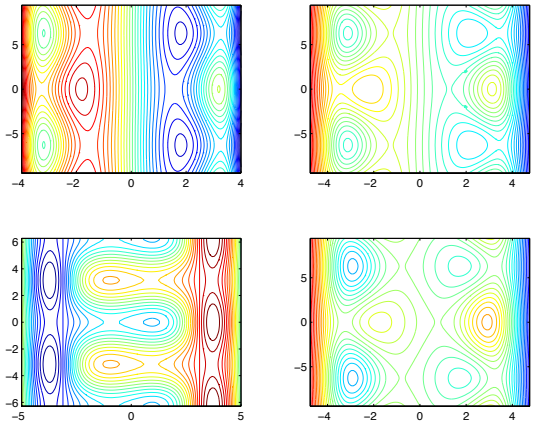

Figure 2: Double separatrix reconnection due to FLR effects with $\rho = 3.25$. Top-left panel double heteroclinic topology; Top-right panel double homoclinic topology; Bottom-left panel heteroclinic-homoclinic topology; Bottom-right panel double reconnection topology;

IV. Shearless transport barrier

FLR can have also a remarkable effect on chaotic transport. In particular, as Fig.3 shows, increasing the Larmor radius can suppress chaotic transport and restore transport barriers that would otherwise be destroyed in the case $\rho = 0$. To quantify this we have performed a numerical study of the destruction of the shear barrier as function of ρ and the perturbation amplitude ε_2. The results are shown in Fig. 4. For each value of ρ there is a critical ε_2 for barrier destruction and this forms a boundary in the $\rho - \varepsilon$ plane as shown in Fig. 4, where red marks indicate where barrier first breaks up and blue means a robust barrier. As anticipated, FLR effects in general restore destroyed barriers but, interestingly, the critical ε_2 is not a monotonic function of ρ. For $\rho \geq 0.5$ barrier is completely restored. The computation of the threshold was performed by following the evolution of the so called indicator points (IP), which are defined as those conforming to the relation, $G_T(x,y) = SI_0(x,y) = (-x, -y + \pi/k_1)$, where G_T is the evolution operator for a time equal to the period of the perturbation T, for the case $k_2 = k_1$ [5]. The symmetry transformations are: $S = \{x' = -x; y' = y + \pi/k_1\}$ and $I_0 = \{x' = x; y' = -y\}$. To find the IP the function $r(x,y) = ||G_T(x,y) - (-x, -y + \pi/k_1||$ is minimized, with the additional condition $r(x,y) = 0$. For our case there is a single IP in the neighborhood of (0,1) whose iteration (Poincaré map) generates the shearless curve (SC) for the corresponding topology. When the perturbation amplitude ε_2 is increased, the SC transits from a 1D curve to a stochastic layer and finally to a chaotic state. The later case is when the transport barrier is destroyed, which we define as the state when the mapping of the IP crosses the unperturbed separatrix ($\varepsilon_2 = 0$) in $3 \cdot 10^4$ iterations.

V. Conclusions

The role of finite Larmor radius effects on chaotic test particle transport was studied in the context of a Hamiltonian dynamical systems. Based on the marginal stability assumption, the Hamiltonian was modeled as the superposition of a non-monotonic zonal shear flow and two regular neutral models of the Hasegawa-Mima equation. FLR effects where incorporated through a gyro-average of the $\mathbf{E}\times\mathbf{B}$ Hamiltonian. This paper has provided numerical evidence of the following novel effects of the role of Larmor radius on chaotic transport: (i) Bifurcation of the zonal flow leading to the creation of additional exrema in the zonal flow profile; (ii) Double heteroclinic-homoclinic separatrix reconnection; and (iii) Chaotic transport suppression and transport barrier restauration.

Acknowledgments Partial support by Conacyt project 81232 and DGAPA-UNAM project IN119408 and from the Oak Ridge National Laboratory, managed by UT-Battelle, LLC, for the U.S. Department of Energy under contract DE-AC05-00OR22725 is acknowledged.

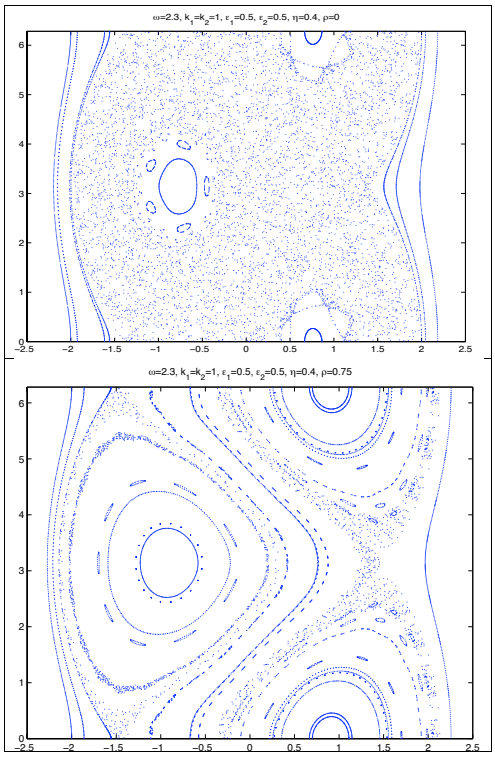

Figure 3: Chaos suppression due to FLR effects for $\omega = 2.3$, $k_1 = k_2 = 2$, $\varepsilon_1 = \varepsilon_2 = 0.5$, η. Top panel, $\rho = 0$. Bottom panel $\rho = 0.75$.

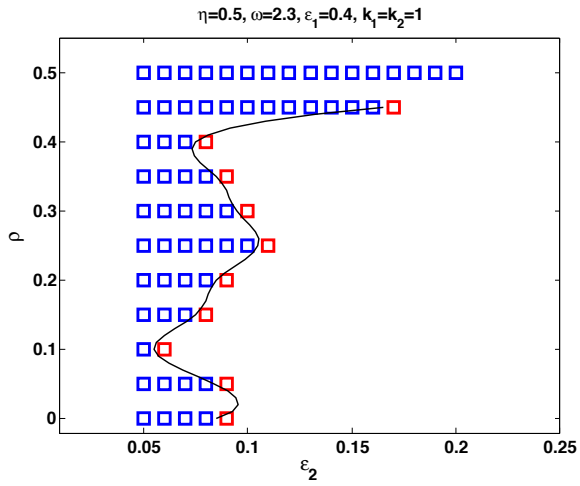

Figure 4: Threshold for transport barrier destruction. At and to the right of the red marks barrier is broken.

References

[1,2] D. del-Castillo-Negrete and P. Morrison, Phys. Fluids A **5**, 948 (1993); D. del-Castillo-Negrete, Phys. Plasmas **7**, 1702 (2000).

[3] del-Castillo-Negrete, Greene, and Morrison, Physica D **91**, 1 (1996).

[4] K. Gustafson, D. del-Castillo-Negrete, and W. Dorland, Phys. of Plasmas **15**, 102309 (2008).

[5] S. Shinohara, and Y. Aizawa, Progress Theor. Phys. **100**, 219 (1998); M.V. Budyansky et al., Phys. Rev. E **79**, 056215 (2010).